Biosensors and Bioelectronics 144 (2019) 111669

Contents lists available at ScienceDirect

Biosensors and Bioelectronics

journal homepage: www.elsevier.com/locate/bios

Ultrasensitive electrochemiluminescence aptasensor for 8-hydroxy-2′-deoxyguanosine detection based on target-induced multi-DNA release and nicking enzyme amplification strategy

Ruo-Nan Zhao, Li-Ping Jia*, Zhe Feng, Rong-Na Ma, Wei Zhang, Lei Shang, Qing-Wang Xue, Huai-Sheng Wang**

Department of Chemistry, Liaocheng University, Liaocheng, Shandong, 252000, China

ARTICLE INFO

Keywords:
8-Hydroxy-2′-deoxyguanosine
Electrochemiluminescence
Aptamer
Signal amplification

ABSTRACT

8-Hydroxy-2′-deoxyguanosine (8-OH-dG) is a principal stable marker of DNA oxidative damage. Sensitive and specific detection of 8-OH-dG is of great importance for early disease diagnosis. In this paper, we developed an electrochemiluminescence aptasensor for 8-OH-dG detection based on target induced multi-DNA release and nicking enzyme signaling amplification strategy. First, three kinds of short DNAs were aligned on the aptamers immobilized on the magnetic beads. In the presence of 8-OH-dG, the aptamer recognized and specifically bound with 8-OH-dG, leading to the release of three kinds of short DNAs and three-fold signal amplification. Then the released short DNAs hybridized with ferrocence (Fc) labeled hairpin DNA (Fc-HP) immobilized on the gold electrode to form a double strand DNA. Subsequently, nicking endonuclease (Nt.*Alw*I) recognized the asymmetric sequence in the dsDNA and cleaved the substrate strand (Fc-HP) into two parts, one fragments containing Fc would leave the surface of electrode. Based on the quenching effect of Fc on the electrochemiluminescence (ECL) of $Ru(bpy)_3^{2+}$/TPA, a signal-on ECL aptasensor was developed. At the same time, three kinds of short DNAs were released again and reused to initiate the repeated cycles of hybridization-cleavage. Under double signal amplification, this aptasensor achieved a low detection of 25 fM and a wide linear range from 100 fM to 10 nM for 8-OH-dG. Besides, the amount of 8-OH-dG in urine samples derived from different people were determined with satisfactory results.

1. Introduction

Oxidative DNA damage, induced by ionizing radiation and other oxygen radical generating systems, is known to involve DNA strand scission, base deletion, and formation of modified DNA bases (Culp et al., 1989). Oxidative DNA damage can contribute to mutation and cancer (Lin et al., 2004a). Although many different oxidative DNA damage products have been identified, 8-hydroxy-2′-deoxyguanosine (8-OH-dG) is the most common oxidative DNA lesion, which takes place by hydroxyl radical attack at the C-8 position of guanine followed by a 1-electron oxidation (Holmberg et al., 1999; Bogdanov et al., 1999). In general, the urinary level range of 8-OH-dG in healthy human is 0 ~ 50 nM (Renner et al., 2000; Wu et al., 2017; Lin et al., 2004b; Svoboda and Kasai, 2004; Lengger et al., 2000). Increasing of 8-OH-dG concentrations can cause a number of disorders including cancer, neurodegenerative diseases and diabetes (Bogdanov et al., 1999). For example, a study showed that the 8-OH-dG level in aqueous humor was higher in patients with age-related macular degeneration, and the level was correlated with the area of macular lesion (Lau et al., 2010). 8-OH-dG is excreted into the urine without further metabolism and its level is not influenced by diet because it is not absorbed through the digestive system. So the urinary level of 8-OH-dG is regarded as an important biomarker of endogenous oxidative damage to DNA (Lin et al., 2004a; Cooke et al., 2002).

The assessment of 8-OH-dG in urine provides a non-invasive approach to evaluate the extent of DNA oxidative damage and repair. At present, chromatography is the most common method to detect 8-OH-dG including high performance liquid chromatography with electrochemical detection (HPLC-ECD) (Pilger et al., 2002; Samcová et al., 2004; Koide et al., 2010), high performance liquid chromatography -coupled mass spectroscopy (HPLC-MS) (Harri et al., 2007; Kataoka et al., 2016), and gas chromatography-coupled mass spectroscopy (GC-

* Corresponding author.
** Corresponding author.
E-mail addresses: jialiping12@l63.com (L.-P. Jia), hswang@lcu.edu.cn (H.-S. Wang).

https://doi.org/10.1016/j.bios.2019.111669
Received 24 June 2019; Received in revised form 25 August 2019; Accepted 30 August 2019
Available online 03 September 2019
0956-5663/

MS) (Lin et al., 2004b). Although HPLC techniques are sensitive for the detection of 8-OH-dG, they often require expensive and time-consuming clean-up procedures before the assay of complex urine samples (Bogdanov et al., 1999). Furthermore, HPLC-MS and GC-MS are limited at present due to its special, high cost and cumbersome equipment. Enzyme-linked immunosorbent assay (ELISA) is another frequently used method to assay 8-OH-dG with high sensitivity and simple instrument (Saito et al., 2000; Chiou et al., 2003). However, this immunoassay might suffer from the questions regarding the specificity (Cooke et al., 2006). Therefore, it is urgent to develop a specific method that is fast, sensitive, simple, selective and cost effective for the determination of trace 8-OH-dG in urine.

Aptamers are DNA or RNA molecules generated through an in vitro selection process called SELEX (Systematic Evolution of Ligand by Exponential enrichment), which possess the ability to recognize various targets such as small molecules, proteins, metal ions and even cell. Currently, hundreds of aptamers have been reported and the aptamer-based biosensors have become attractive in analytical applications because of its advantages such as cheap, easy synthesis and labeling, thermal and chemical stability (Gómez et al., 2019). The unique nucleic acids structure of aptamer can transform the detection of target to a nucleic acid quantification event, and this allows the use of different nucleic acid amplification strategies to improve the sensitivity of the biosensor (Gómez et al., 2019; Li et al., 2015). A variety of amplification techniques have been employed to improve the sensitivity including polymerase chain reaction (PCR), rolling circle amplification (RCA) (Zhu et al., 2016), strand displacement amplification (SDA) (He et al., 2012), hybridization chain reaction (HCR) (Bi et al., 2017), exonuclease-assisted signal amplification (Lin et al., 2018; Huang et al., 2016), and nicking endonuclease-assisted signal amplification (NESA) (Yao et al., 2015). Specifically, NESA has become a novel isothermal amplification tool in recent years. NESA assays mainly involve the use of specific nicking enzymes that can recognize specific sequences on double stranded DNA and cleave only one strand at that restriction site (Gómez et al., 2019; Li et al., 2015). NESA assays can achieve exponentially amplification by the cleavage of probe and release of the target DNA. Aptamers can be used in NESA assays to detect targets other than nucleic acids. The key for the fabrication of aptasensor based on NESA assays is how to establish the relationship between aptamer and recognition sequence.

In recent years, electrochemiluminescence (ECL) detection has attracted wide interests due to its outstanding characteristics including simple equipment, low cost, high sensitivity, and low background (Li et al., 2016). Among various ECL systems, ECL based on tris(2, 2′-bipyridyl) ruthenium(II) ($Ru(bpy)_3^{2+}$) is well received owing to its easy operation, high sensitivity, and excellent stability (Zhang et al., 2016). Cao et al. reported that ferrocene (Fc) molecule can efficiently quench ECL of $Ru(bpy)_3^{2+}$ (Cao et al., 2006). Wu et al. established an ECL sensing platform for the detection of adenosine based on Fc-labeled structure-switching signaling aptamer (Wu et al., 2013). In the present work, we developed an 'signal-on" ECL aptasensor for 8-OH-dG detection based on the structure-switching of Fc-labeled hairpin DNA (Fc-HP) immobilized on gold electrode (Scheme 1). Unlike most electrochemical aptasensors prepared by directly immobilizing aptamer on the electrode surface, we firstly connected 8-OH-dG aptamer with magnetic beads by amide bond. Then every aptamer hybridized with three kinds of short DNA strands (P1, P2, P3), which consisted of two parts: one complementary to aptamer and another to Fc-HP. In the presence of 8-OH-dG, three kinds of short DNAs were released again due to the affinity between aptamer and target. After magnetic separation, the released short DNAs were left in the supernatant. In the next procedure, the released short DNAs hybridized with Fc-HP immobilized on gold electrode to form double DNA strands. In the presence of nicking endonuclease (Nt.*Alw*I), Fc-HP would be cleaved into two parts and one part containing Fc would leave the surface of electrode. Meanwhile, three kinds of short DNAs were released and then hybridized with another Fc-HP to initiate a new cycle of nicking endonuclease cleavage reaction. Because of nicking endonuclease-assisted recycling amplification, more Fc would leave the surface of the gold electrode. Accordingly, the ECL intensity of $Ru(bpy)_3^{2+}$/TPA system would be enhanced greatly and the detection sensitivity would be improved. The fabricated aptasensor possessed two merits: First, every long aptamer hybridized with three kinds of short DNAs, one biological binding event would cause the release of three kinds of DNAs simultaneously, and as a result, triple the signal would be amplified. Second, nicking endonuclease-assisted amplification strategy realized the recycling of three kinds of short DNAs, which greatly improved the detection sensitivity. With such design, the ECL aptasensor achieved an ultrasensitive response to 8-OH-dG, indicating a promising potential for evaluation of oxidative DNA damage.

2. Experimental

2.1. Materials and reagents

All oligonucleotides used in the experiment were synthesized by Sangon Biotechnology Co., Ltd. (Shanghai, China), and their sequences were listed in Table S1. The nicking enzyme (Nt.*Alw*I, 10000 U/mL) and 10× NEB buffer (500 mM NaCl, 100 mM Tris-HCl, 100 mM $MgCl_2$, and 10 mM dithiothreitol, pH 7.9) were purchased from the New England Biolabs (Ipswich, U.S.A.). 8-Hydroxy-2′-deoxyguanosine (8-OH-dG), guanine, and guanosine were purchased from Sigma-Aldrich. Uric acid, urea, ascorbic acid, tris-(hydroxymethyl)-aminomethane (Tris), tris-(2-carboxyethyl)-phosphine hydrochloride (TCEP), 6-mercapto-1-hexanol (MCH), and carboxylated Fe_3O_4 magnetic beads were purchased from Aladdin Inc. (Shanghai, China). Tris (2,2′-bipyridyl) ruthenium (II) chloride hexahydrate ($Ru(bpy)_3^{2+}$), N-(3-(dimethylamino) propyl)-N′-ethylcarbodiimide hydro-chloride (EDC), and N-hydroxysuccinimide (NHS) were purchased from Alfa Aesar. Tri-n-propylamine (TPA) was purchased from Shanghai Macklin Biochemical Co., Ltd. Other reagents such as NaCl, $Zn(NO_3)_2$, $MgCl_2$, $Cu(NO_3)_2$ were purchased from Shanghai Reagent Corporation (Shanghai, China). All these reagents were of analytical grade and without further purification. DNA was stored in Tris-HCl (10 mM, pH 8.0) containing 1.0 mM EDTA. Tris-HCl buffer (10 mM, pH 7.4) containing 100 mM NaCl and 5 mM $MgCl_2$ was employed for hybridizing and washing. Furthermore, the thiolated Fc-HP was reduced in 2 mM TCEP for 1 h to cleave disulfide bonds, respectively. All solutions were prepared with Milli-Q water (18 mΩ cm resistivity) from a Millipore system.

2.2. Preparation of aptamer-modified magnetic beads

Aptamer－modified magnetic beads were prepared as reported previously (Dong et al., 2018). 100 μL of 5 mg mL^{-1} carboxylated magnetic beads (MBs) were washed three times with 0.5 mL imidazole-HCl buffer (pH 7.4). Then MBs were activated in 200 μL of 0.1 M imidazole-HCl buffer containing 10 mg of NHS and 20 mg of EDC for 1 h with shaking at room temperature. After that, 5 μL of 100 μM amino-modified aptamer was added into the activated MBs solution, the mixture reacted for 12 h at 37 °C to form aptamer-MBs (Fig. S1 showed the aptamers were mainly bound to MBs by amide bond and the non-specific adsorption was small). After being separated and washed with imidazole-HCl buffer, the aptamer-MBs immersed in 3% BSA solutions for 1 h at 37 °C to remove the nonspecific sites. Then the aptamer-MBs was redispersed in 200 μL of PBS buffer (0.1 M, pH 7.4) after separation and wash. Next, 150 μL of three kinds of short DNAs (P1, P2, P3, 10 μM for each) was added to the above solution incubating for 2 h at 37 °C. After being washed with PBS buffer, the final P1/P2/P3-aptamer-MBs complex was redispersed in 200 μL of PBS buffer and stored in a refrigerator at 4 °C for further use.

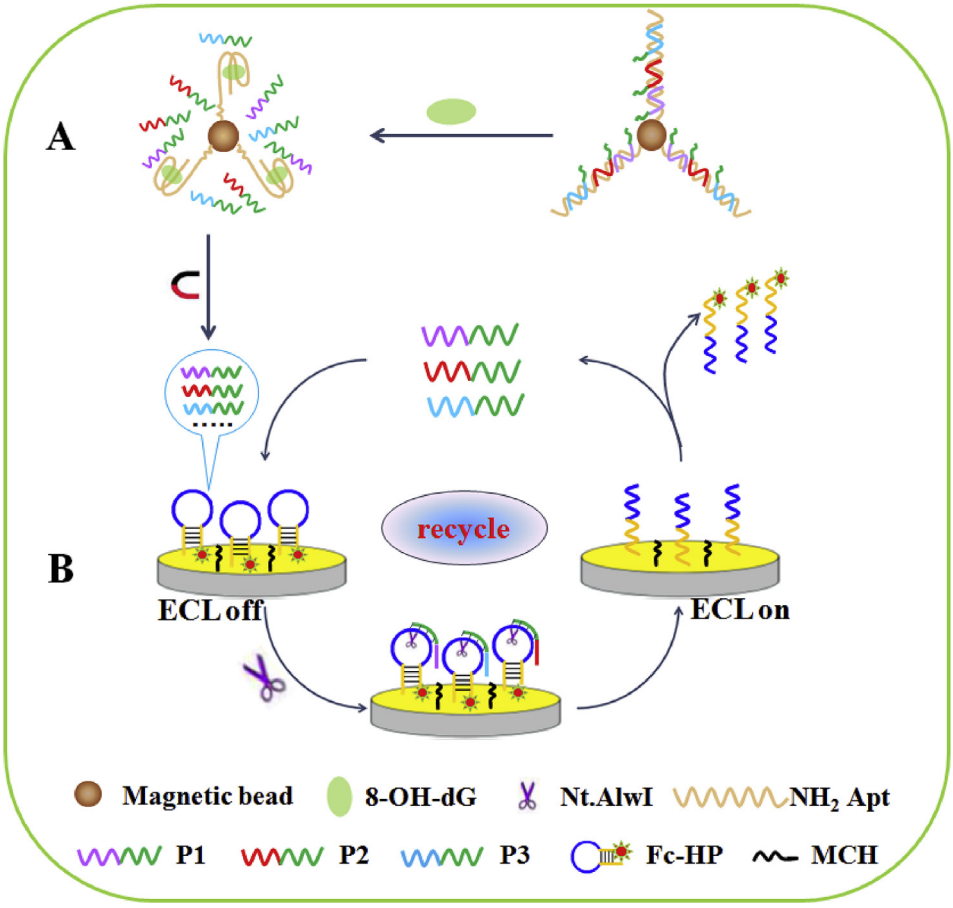

Scheme 1. Design strategy of the ECL aptasensor. (A) Aptamer recognition and release of three short DNAs. (B) ECL detection principle for 8-OH-dG.

2.3. Fabrication of ECL aptasensor

A gold electrode (2 mm in diameter) was polished on a microcloth with 0.05 μm alumina slurry for 5 min, followed by sonicating in ethanol and water for 5 min, respectively. Then the polished electrode was electrochemically cleaned in 0.5 M H_2SO_4 solution by scanning from -0.3 V to +1.5 V until a steady-state cyclic voltammogram was obtained. After being thoroughly rinsed with Milli-Q water and dried with nitrogen, 5 μL of 0.2 μM Fc-HP was dropped on the cleaned electrode surface for incubating 2.5 h at 37 °C. After that, 6 μL of 1 mM MCH was dropped on the Fc-HP modified electrode for 0.5 h at room temperature to block the unoccupied surface binding sites. The obtained MCH/Fc-HP modified electrode was used to the hybridization with P1, P2 and P3.

Next, different concentrations of 8-OH-dG were mixed with 5 μL P1/P2/P3-aptamer-MBs suspension. Then the mixture was diluted to 10 μL with PBS buffer and reacted for 2 h at 37 °C to release three kinds of short DNAs. The released short DNAs were left in the supernatant after magnetic separation. 5 μL of the supernatant was dropped on the MCH/Fc-HP modified electrode incubating for 1 h at 37 °C. Subsequently, the electrode was treated with 5 μL of 10 U Nt.*AlwI* for 1.5 h at 37 °C. After each modification step, the electrode surface was washed with 10 mM Tris-HCl buffer (pH 7.4) and dried with nitrogen. Finally, the electrode was placed in 5 mL of PBS (pH 7.4) containing 10 mM $LiClO_4$, 0.4 mM $Ru(bpy)_3^{2+}$ and 0.06 mM TPA to perform the ECL measurements.

2.4. Electrochemical and electrochemiluminescence detection

All electrochemical experiments were performed with a CHI 760C electrochemical workstation (CH Instruments, Shanghai, China) with a conventional three-electrode system comprising a gold working electrode, a platinum wire auxiliary electrode, and a Ag/AgCl reference electrode. ECL was recorded with an electrogenerated chemiluminescence analyzer (Xi'an Remax Tech. Co. Ltd.). Electrochemical impedance spectroscopy (EIS) was carried out in 5 mM $[Fe(CN)_6]^{3-/4-}$ solution containing 0.1 M KCl with the frequency range from 0.1 Hz to 10 kHz. The amplitude of the applied sine wave potential was 5 mV and the formal potential of the system was set at +0.22 V. The ECL measurement was performed with cyclic voltammogram at a potential ranging from 0.0 V to 1.2 V at a scan rate of 100 mV s^{-1} in 5.0 mL of PBS (pH 7.4) solution containing 10 mM $LiClO_4$, 0.4 mM $Ru(bpy)_3^{2+}$ and 0.06 mM TPA with a conventional three-electrode system. The photomultiplier tube (PMT) was set at +800 V.

3. Results and discussion

3.1. Feasibility of the ECL aptasensor

The polyacrylamide gel electrophoresis (PAGE) was used to characterize the hybridization between aptamer and three kinds of short DNAs. As shown in Fig. S2, lanes 1, 2, 3 and 4 showed the GE results for P1, P2, P3 and aptamer, respectively. Because the P2 and aptamer sequence easily form dipolymer, two distinct bright bands were observed (lane 2 and 4). Lane 5 exhibited a distinct band at the top of the strip, indicating the formation of aptamer – three short DNAs complexes.

The feasibility of the proposed ECL aptasensor was confirmed by EIS and ECL measurements. In a typical EIS, the diameter of semicircle equals to the electron-transfer resistance, which reflects the electron transfer kinetics of the redox probe ($[Fe(CN)_6]^{3-/4-}$) at the electrode surface. As shown in Fig. 1A, a very small semicircle was observed for

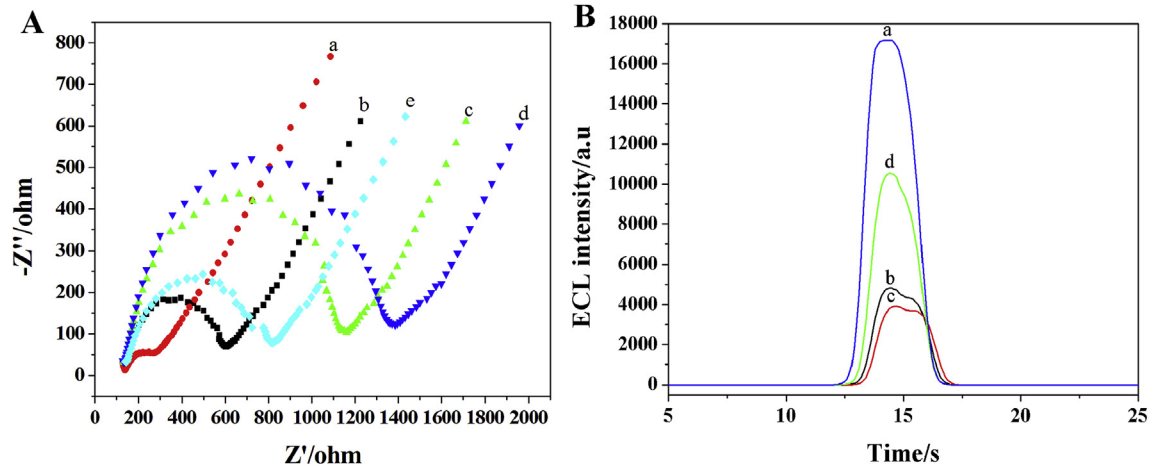

Fig. 1. (A) EIS of gold electrode at different stages: (a) bare Au electrode, (b) Fc-HP/Au, (c) MCH/Fc-HP/Au, (d) P1/P2/P3/MCH/Fc-HP/Au, (e) nicking of electrode d by Nt.*Alw*I. (B) ECL response of bare electrode (a), MCH/Fc-HP/Au (b), P1/P2/P3/MCH/Fc-HP/Au before (c) and after nicking by Nt.*Alw*I (d) in $Ru(bpy)_3^{2+}$/TPA solutions. (For interpretation of the references to color in this figure legend, the reader is referred to the Web version of this article.)

bare gold electrode (curve *a*), indicating a fast electron-transfer process of $Fe(CN)_6^{3-/4-}$ redox system. The resistance increased with the immobilization of Fc-HP on the gold electrode surface (curve b) due to the effective repulsion between the negatively phosphate structure of DNA and $Fe(CN)_6^{3-/4-}$ anions. Subsequent surface blocking with 6-mercaptohexanol (MCH) also led to an obvious increase in resistant (curve c). After hybridization with released three short DNAs (P1, P2, P3), the resistance increased furtherly (curve d). After nicking by Nt.*Alw*I, the resistant decreased greatly (curve e) because Fc-HP strands were cleaved two parts by nicking endonuclease cyclically, only leaving one part on the electrode.

Fig. 1B showed the ECL intensity of the proposed aptasensor at different modification stages. $Ru(bpy)_3^{2+}$/TPA system exhibited a strong ECL peak at bare gold electrode (curve a). However, the ECL intensity decreased greatly when Fc-HP was captured on electrode surface (curve b). As shown in Fig. S3, the ECL intensity of the $Ru(bpy)_3^{2+}$/TPA system had no obvious decrease when HP was captured on electrode surface, indicating that the ECL quenching of $Ru(bpy)_3^{2+}$ was mainly caused by Fc. The ECL quenching effect of $Ru(bpy)_3^{2+}$/TPA by Fc has been well studied in previous study (Cao et al., 2006). After Fc-HP hybridizing with released short DNAs (P1, P2, P3), the ECL decreased slightly (curve c). Interesting, after nicking endonuclease was incubated on the P1/P2/P3/MCH/Fc-HP/Au sensing surface, the ECL intensity recovered significantly (curve d). However, in another control experiment (shown in Fig. S3, only Fc-HP was replaced with HP under same experimental conditions), the ECL intensity changed slightly (curve c and d in Fig. S3) before and after nicking endonuclease incubation. The results indicated that the change of ECL of $Ru(bpy)_3^{2+}$/TPA mainly resulted from structure-switching of Fc-HP. With the increasing of 8-OH-dG concentration, the ECL intensity would increase due to more short DNAs were released and more Fc-HP were cleaved. Therefore, 8-OH-dG can be detected quantitatively through the change of ECL intensity of $Ru(bpy)_3^{2+}$/TPA.

3.2. Experimental optimization of the ECL aptasensor

In order to obtain the best performance for the detection of 8-OH-dG, the experimental conditions such as the number of DNAs aligned on a single aptamer, the concentration and incubation time of Fc-HP on electrode, the reaction time of 8-OH-dG with aptamer, and the incubation time of nicking endonuclease were investigated with 50 pM 8-OH-dG. In general, one aptamer recognizes specific target to release a single DNA. However, in this work, three kinds of short DNAs all partly hybridized with one aptamer sequence were used to amplify the signal. In order to prove the amplification effect of using three kinds of DNAs, the ECL intensity with one and three kinds of DNAs in a single aptamer strand were studied. As shown in Fig. S4, the ECL intensity using three kinds of DNAs was much higher than that using one kinds, indicating that multi-kinds of DNAs hybridization systems would result in more DNAs being released and then more Fc-HP being cleaved, which was beneficial for the recovery of ECL.

As shown in Fig. S5A, the ECL intensities of $Ru(bpy)_3^{2+}$ decreased with increasing the concentration of Fc-HP from 0.5 to 2.0 μM, indicating more Fc-HP immobilized on the electrode. However, the ECL intensities of $Ru(bpy)_3^{2+}$ changed slightly when the concentrations of Fc-HP were higher than 2.0 μM, indicating that the quantity of Fc-HP on the electrode had reached saturate. Furthermore, the ECL intensities of $Ru(bpy)_3^{2+}$ decreased firstly with increasing incubation time of Fc-HP on the electrode from 1.5 to 2.5 h and then did not change obviously (Inset of Fig. S5A). So 2.0 μM Fc-HP and 2.5 h incubation time were chosen in the following experiments. In the present work, there was a binding competition between 8-OH-dG and three kinds of short DNAs with aptamer, so the reaction time of 8-OH-dG with aptamer was very important. As shown in Fig. S5B, the ECL intensities increased gradually from 20 to 60 min and afterward reached a stable value. This is because more short DNAs could be released to hybridize with Fc-HP immobilized on electrode with extending reaction time, resulting in more Fc-HP being cleaved and ECL recovery. So 60 min was selected as the optimum reaction time. Furthermore, the effect of the reaction time of the nicking reaction on the ECL signal was investigated too. As shown in Fig. S5C, the ECL signal increased with increasing reaction time and reached a plateau after 1.5 h. Therefore, 1.5 h was chosen as the optimized time in the following study.

3.3. Calibration curves of the ECL aptasensor

Under optimized experiment conditions, the ECL aptasensor was applied to detect 8-OH-dG with different concentrations. As shown in Fig. 2A, ECL intensities of $Ru(bpy)_3^{2+}$/TPA system increased gradually with increasing 8-OH-dG concentrations. The ECL peak intensities showed a linear range with logarithm of 8-OH-dG concentrations from 100 fM to 10 nM. The linear equation was $I_{ECL} = 729.70 + 2271.80 \lg c$/fM with a correlation coefficient of $R = 0.9935$. The estimated detection limit (defined as $DL = 3\sigma/S$, where σ is the standard deviation of the blank and S is the slope of the corresponding calibration curve) was 25 fM. Compared with reported methods for the detection of 8-OH-dG (Table 1), this ECL aptasensor showed lower detection limit and wider linear range.

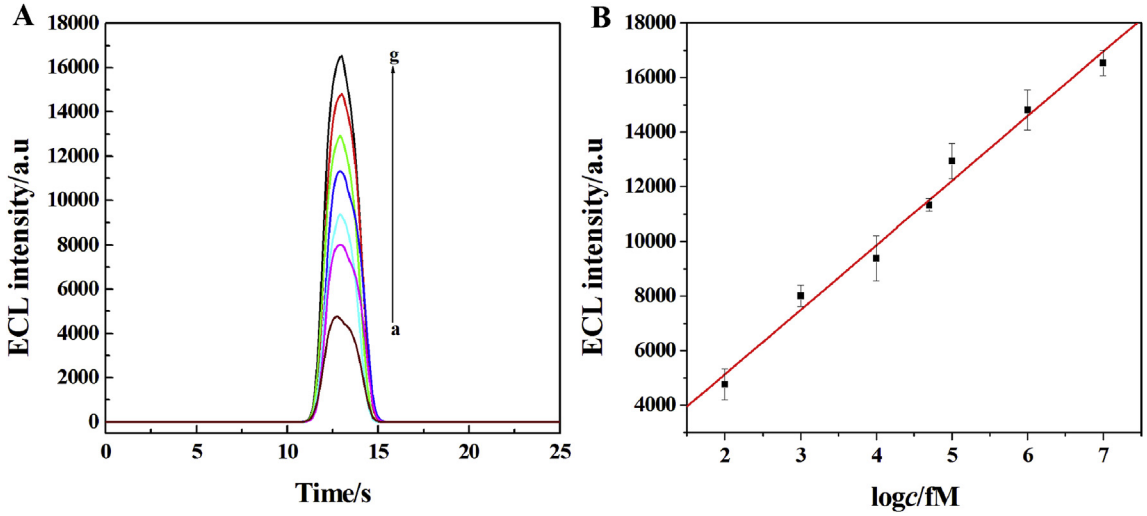

Fig. 2. (A) ECL responses of the aptasensor in the presence of different concentrations of 8-OH-dG (from a to g: 100 fM, 1 pM, 10 pM, 50 pM, 100 pM, 1 nM, 10 nM). (B) Calibration plots of ECL peak intensity vs. the logarithm of the 8-OH-dG concentration (fM). Error bars show the standard deviations for three independent experiments.

Table 1
Comparison of various methods for 8-OH-dG detection.

Method	LOD	Linear range	Reference
Electrochemistry	31.3 nM	0.5 μM–35 μM	Sun et al. (2015)
Electrochemistry	18.8 nM	0.0563 μM–16.4 μM	Guo et al. (2016)
Electrochemistry	0.875 nM	5.6 nM – 1155nM	Jia et al. (2015)
HPLC – MS/MS	0.5 nM		Weimann et al. (2002)
CE – ECD	2.6 nM	0.01 – 1.5 μM	Zhang et al. (2010)
ECL immunosensor	0.3 nM	0.7-700 nM	Zhang et al. (2015)
colorimetric aptasensor	141 pM	0.466 - 247 nM	Liu et al. (2014)
CD spectra	33 pM	0.05 nM–2 nM	Liu et al. (2016)
RLS spectra	27.3 pM	90.8 pM - 14.1 nM	Guo et al. (2012)
Electroaptasensor	2.7 pM	10 pM - 100 μM	Jia et al. (2018)
ECL aptasensor	38.8 aM	50 aM - 1 fM	Lv et al. (2018)
ECL aptasensor	**25 fM**	**100 fM-10 nM**	**Present work**

3.4. Performance of the ECL biosensor

Some important performances, such as selectivity, stability, and reproducibility of this proposed ECL aptasensor were investigated. As depicted in Fig. 3A, the influence of some inorganic and organic compounds on the ECL intensity of the prepared aptasensor was investigated. When the developed aptasensor was treated with 100 nM Zn^{2+}, Cu^{2+}, Mg^{2+}, Na^{+}, uric acid, ascorbic acid, guanosine, guanine, respectively, there were no remarkable enhancements in ECL signal, which were nearly closed to the blank PBS solution. In contrast, the ECL intensity obtained from 50 pM 8-OH-dG increased dramatically, indicating the aptasensor displayed favorable selectivity in detecting 8-OH-dG even in the complicated matrix with above interference reagents.

Furthermore, the stability and reproducibility of the aptasensor were further testified. As seen in Fig. 3B, ECL intensities obtained from blank and 50 pM 8-OH-dG under continuous potential scanning of fourteen cycles showed a relatively stable signal. The relative standard deviations (RSD) from blank and 50 pM 8-OH-dG were 1.28% and 1.78%, respectively. For the reproducibility, five of the proposed aptasensors with 50 pM 8-OH-dG prepared in parallel were examined under the same experimental conditions. And the RSD was 4.22%, indicating an acceptable reproducibility for detection of 8-OH-dG. As a consequence, the proposed biosensor exhibited excellent selectivity, stability and reproducibility for 8-OH-dG assay.

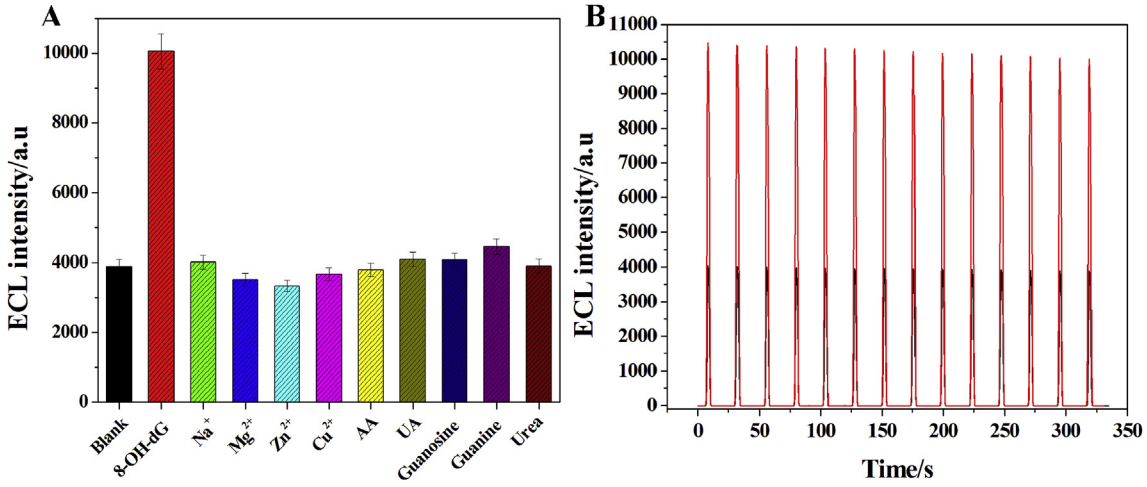

Fig. 3. (A) Specificity of the proposed aptasensor toward different interfering substances. Error bars show the standard deviations for three independent experiments. (B) Stability of the aptasensor in the absence (black line) and presence of 50 pM 8-OH-dG (red line). (For interpretation of the references to color in this figure legend, the reader is referred to the Web version of this article.)

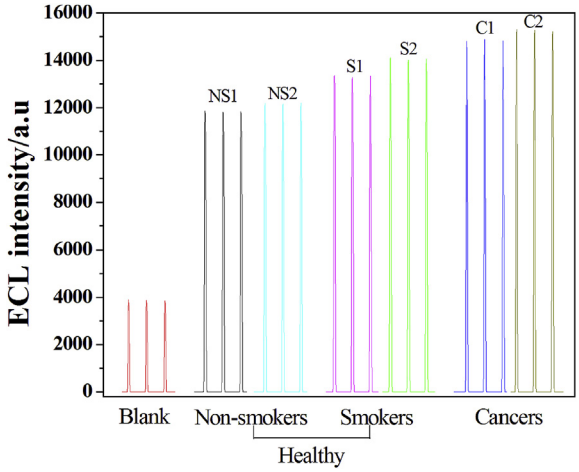

Fig. 4. ECL responses of the aptasensor for different urine samples.

3.5. Real sample analysis

In order to examine the availability of the proposed aptasensor, we challenged our ECL sensor in urine samples for the detection of 8-OH-dG. Two urine samples from cancer patient were collected from hospital and other four urine samples including two non-smokers and two smokers were obtained from healthy volunteers. The urine samples were analyzed with the developed method after being diluted in 1:10 ratio with PBS buffer. Recovery test was carried out by adding a known amount of 8-OH-dG to the urine samples. Fig. 4 shows the detection results of 8-OH-dG in urine from different peoples. The ECL intensities obtained from smoker urine samples are higher than those from non-smokers, indicating that cigarette smoking would induce oxidative damage to DNA and 8-OH-dG had a high expression level in smoker urine. The results were in agreement with others in the literature (Yao et al., 2004; Honda et al., 2000; Asami et al., 1997). Moreover, samples from cancer patients were analyzed. It was observed that the urinal level of 8-OHdG was significantly increased in cancer patients than that in healthy peoples. Previous studies (Kuo et al., 2007; Yano et al., 2009; Guo et al., 2017) found that the urine levels of 8-OH-dG were significantly higher in patients with cancer compared with healthy peoples, which supports our findings. The concentrations of 8-OH-dG in urine and the recoveries were calculated and the results were listed in Table S2. As shown in Table S2, the concentrations of 8-OH-dG in urine of cancer patients were distinctly higher than those of the healthy peoples. This study indicated that 8-OH-dG can be considered as a promising biomarker for the early detection and diagnosis of some diseases related to DNA oxidative damage and oxygen radical. Furthermore, the concentrations of 8-OH-dG obtained with this ECL aptasensor were consistent with those determined by ELISA method. These results indicated that this fabricated ECL aptasensor can detect 8-OH-dG in urine samples with high accuracy.

4. Conclusion

Inspired by the quenching effect of Fc on the ECL of $Ru(bpy)_3^{2+}$/TPA, we developed a signal-on ECL aptasensor for highly sensitive and specific detection of 8-OH-dG. In order to promote the sensitivity of the aptasensor, a dual signal amplification strategy was used in this study. First, three kinds of short DNAs were aligned on the 8-OH-dG aptamers modified on magnetic beads. In the presence of 8-OH-dG, the aptamer would bind to 8-OH-dG, and one biological binding event would cause the release of three kinds of DNAs simultaneously, resulting in the first amplification. Second, the released DNAs were introduced into the nicking endonuclease-assisted cyclic enzymatic amplification to cleave more Fc-HP, resulting in the significant ECL recovery. Under dual signal amplification, this aptasensor can determine 8-OH-dG as low as 25 fM with a linear range of 100 fM - 10 nM. More importantly, this ECL aptasensor has been successfully applied in complex matrix of urine from different peoples with the good accuracy and precision, which indicated that this method has huge potential in clinical diagnosis and disease prevention.

CRediT authorship contribution statement

Ruo-Nan Zhao: Data curation, Formal analysis, Writing - original draft, Writing - review & editing. **Li-Ping Jia:** Formal analysis, Writing - review & editing, Writing - review & editing, Writing - review & editing, Formal analysis, Writing - review & editing. **Zhe Feng:** Writing - review & editing. **Rong-Na Ma:** Writing - review & editing. **Wei Zhang:** Formal analysis. **Lei Shang:** Writing - review & editing. **Qing-Wang Xue:** Writing - review & editing.

Declaration of competing interest

The authors declare that they have no known competing financial interests or personal relationships that could have appeared to influence the work reported in this paper.

Acknowledgement

This work is supported by the National Natural Science Foundation of China (No. 21405070, 21427808, 21505063 & 21375055).

Appendix A. Supplementary data

Supplementary data to this article can be found online at https://doi.org/10.1016/j.bios.2019.111669.

References

Asami, S., Manabe, H., Miyake, J., Tsurudome, Y., Hirano, T., Yamaguchi, R., Itoh, H., Kasai, H., 1997. Carcinogenesis 18 (9), 1763–1766.
Bi, S., Yue, S., Zhang, S., 2017. Chem. Soc. Rev. 46, 4281–4298.
Bogdanov, M.B., Beal, M.F., McCabe, D.R., Griffin, R.M., Matson, W.R., 1999. Free Radical Biol. Med. 27, 647–666.
Cao, W., Ferrance, J.P., Demas, J., Landers, J.P., 2006. J. Am. Chem. Soc. 128 (23), 7572–7578.
Chiou, C.C., Chang, P.Y., Chan, E.C., Wu, T.L., Tsao, K.C., Wu, J.T., 2003. Clin. Chim. Acta 334, 87–94.
Cooke, M.S., Evans, M.D., Lunec, J., 2002. Free Radic. Res. 36, 929–932.
Cooke, M.S., Singh, R., Hall, G.K., Mistry, V., Duarte, T.L., Farmer, P.B., Evans, M.D., 2006. Free Radic. Biol. Med. 41, 1829–1836.
Culp, S.J., Cho, B.P., Kadlubar, F.F., Evans, F.E., 1989. Chem. Res. Tonicol. 2, 416–422.
Dong, H., Chen, H., Jiang, J., Zhang, H., Cai, C., Shen, Q., 2018. Anal. Chem. 90, 4507–4513.
Gómez, R.L., Castro, R.M., Álvarez, N.S., Castañón, M.J.L., 2019. Curr. Opin. Electrochem. 14, 32–43.
Guo, C., Li, X.F., Ye, M.F., Xu, F., Yu, J.K., Xie, C., Cao, X.J., Guo, M.Z., Yuan, Y., Zheng, S., 2017. Oncotarget 8, 53100–53109.
Guo, H., Xue, K., Yan, L., 2012. Sens. Actuators B Chem. 171–172, 1038–1045.
Guo, Z., Liu, X., Liu, Y., Wu, G., Lu, X., 2016. Biosens. Bioelectron. 86, 671–676.
Harri, M., Kasai, H., Mori, T., Tornaeusa, J., Savela, K., Peltonen, K., 2007. J. Chromatogr. B 853, 242–246.
He, Y., Li, W., Nie, Z., 2012. Chem. Eur J. 18, 3992–3999.
Holmberg, I., Stal, P., Hamberg, M., 1999. Free Radic. Biol. Med. 26 (1/2), 129–135.
Honda, M., Yamada, Y., Tomonaga, M., Ichinose, H., Kamihira, S., 2000. Leuk. Res. 24, 461–468.
Huang, K., Shuai, H., Zhang, J., 2016. Biosens. Bioelectron. 77, 69–75.
Jia, L., Liu, J., Wang, H., 2015. Biosens. Bioelectron. 67, 139–145.
Jia, L., Wang, L., Ma, R., Shang, L., Zhang, Wei, Xue, Q., Wang, H., 2018. Talanta 179, 414–419.
Kataoka, H., Mizuno, K., Oda, E., Saito, A., 2016. J. Chromatogr. B 1019, 140–146.
Koide, S., Kinoshita, Y., Ito, N., Kimura, J., Yokoyama, K., Karube, I., 2010. J. Chromatogr. B 878, 2163–2167.
Kuo, H.W., Chou, S.Y., Hu, T.W., Wu, F.Y., Chen, D.J., 2007. Mutat. Res. 631, 62–68.
Lau, L., Liu, C., Wei, Y., 2010. Investig. Ophthalmol. Vis. Sci. 51, 5486–5490.
Lengger, C., Schöch, G., Topp, H., 2000. Anal. Biochem. 287, 65–72.
Li, F., Zhang, H., Wang, Z., Newbigging, A.M., Reid, M.S., Li, X., Le, X., 2015. Anal. Chem. 87, 274–292.
Li, S.K., Chen, A.Y., Chai, Y.Q., Yuan, R., Zhuo, Y., 2016. Electrochem. Acta. 212,

767–774.
Lin, C., Zheng, H., Huang, Y., Chen, Z., Luo, F., Wang, J., Guo, L., Qiu, B., Lin, Z., Yang, H., 2018. Biosens. Bioelectron. 117, 474–479.
Lin, H., Jenner, A.M., Ong, C.N., Huang, S., Whiteman, M., Halliwell, B., 2004a. Biochem. J. 380, 541–548.
Lin, H.S., Jenner, A.M., Ong, C.N., Huang, S.H., Whiteman, M., Halliwell, B., 2004b. Biochem. J. 380, 541–548.
Liu, H., Wang, Y., Wang, J., Xue, J., Zhou, B., Zhao, H., Liu, S., Tang, X., Chen, S., Li, M., Cao, J., 2014. Anal. Biochem. 458, 4–10.
Liu, Y., Wei, M., Zhang, L., Zhang, Y., Wei, W., Yin, L., Pu, Y., Liu, S., 2016. Anal. Chem. 88, 6509–6514.
Lv, Y., Chen, S., Shen, Y., Ji, J., Zhou, Q., Liu, S., Zhang, Y., 2018. J. Am. Chem. Soc. 140, 2801–2804.
Pilger, V., Ivancsits, S., Germadnik, D., Rüdige, H.W., 2002. J. Chromatogr. B 778, 393–401.
Renner, T., Fechner, T., Scherer, G., 2000. J. Chromatogr. B 738, 311–317.
Saito, S., Yamauchi, H., Hasui, Y., Kurashige, J., Ochi, H., Yoshida, K., 2000. Res. Commun. Mol. Pathol. Pharmacol. 107, 39–44.
Samcová, E., Marhol, P., Opekar, F., Langmaier, J., 2004. Anal. Chim. Acta 516, 107–110.
Sun, X., Zhang, L., Zhang, H., Qian, H., Ji, J., Tang, L., Li, Z., Zhang, G., 2015. Anal. Methods. 7, 6664–6671.
Svoboda, P., Kasai, H., 2004. Anal. Biochem. 334, 239–250.
Weimann, A., Belling, D., Poulsen, H.E., 2002. Nucleic Acids Res. 30, E7.
Wu, D.N., Liu, B.D., Yin, J.F., Xu, T., Zhao, S.L., Xu, Q., Chen, X., Wang, H.L., 2017. J. Chromatogr. B 1064, 1–6.
Wu, M.S., Yuan, D.J., Xu, J.J., Chen, H.Y., 2013. Anal. Chem. 85, 11960–11965.
Yano, T., Shoji, F., Baba, H., Koga, T., Shiraishi, T., Orita, H., Kohno, H., 2009. Lung Cancer 63, 111–114.
Yao, Q., Mei, S., Weng, Q., Zhang, P., Yang, Q., Wu, C., Xu, G., 2004. Talanta 63, 617–623.
Yao, G., Liang, R., Yu, X., Huang, C., Zhang, L., Qiu, J., 2015. Anal. Chem. 87, 929–936.
Zhang, A., Miao, C., Shi, H., Xiang, H., Huang, C., Jia, N., 2016. Sens. Actuators B Chem. 222, 433–439.
Zhang, S., Zou, C., Luo, N., Weng, Q., Cai, L., Wu, C., Xing, J., 2010. Chem. Lett. 21, 85–88.
Zhang, T., Zhao, H., Fan, X., Chen, S., Quan, X., 2015. Talanta 131, 379–385.
Zhu, Y., Wang, H., Wang, L., Zhu, J., Jiang, W., 2016. ACS Appl. Mater. Interfaces 8, 2573–2581.